MODELING ENERGY AND STRESS CONCENTRATION IN DIESEL ENGINES WITH FLEXIBLE CRANKSHAFT

Salah Almoslehy[1,2]* – Yaser Hadi[3]

[1]CFisUC, Department of Physics, University of Coimbra, P-3004 516 Coimbra, Portugal
[2]Faculty of Engineering, Xiamen University of Technology (XMUT), No. 600 Ligong Road, Jimei, Xiamen 361024, China
[3]Department of Mechanical Engineering Technology, Yanbu Industrial College, Yanbu, Kingdom of Saudi Arabia

Abstract:

Diesel engines feature significant power but result in huge dynamics that is related to the flexibility of crankshaft. Such flexibility decreases the air mass flow rate, resulting in a higher rate of CO exhaust emission. Since the analytical modeling of such dynamics has not been done yet, the present paper investigates the strain energy-based aspects, frequency-related aspects and stress concentration in diesel engines with flexible crankshaft. The result shows that the most influential parameters onto the strain energy of flexible crankshafts are the mass moment of inertia and the distance between the crank and the bearing of crankshaft. The radial force is several times larger than the tangential force. The force due to cylinder's pressure is several times larger than the force due to inertia, which is in turn several times larger than the force due to eccentricity. The study remedies the stress concentration in crankshaft by identifying: (i) the location of the most critical section of stress concentration, (ii) the effect of the radius of the crankpin shoulder fillet on the maximum shearing stress and maximum bending stress that can be withstood by the crankpin. The study facilitates determining the value of the radius of the crankpin shoulder fillet that remedies the stress concentration in the most critical section in crankshaft. The paper formulates the stress concentration factor and provides the sensitivity analysis thereon. The proposed models enable better performance of diesel engines, prolonging their service life and improving air quality.

1   Introduction

Although it is an old invention, crankshaft is still in use in internal combustion engines extensively today. Since diesel engines feature distinguished performance and modeling is a key tool in vehicular systems development, modeling plays a key role in diesel engine development [1]. Analytical / semi-analytical models are critically significant since they provide the basis of the core and subroutines of computational modelers. In addition, analytical modeling brings about the following advantages over the real engines testing: (a) A self-validated model of the real engine with physically explainable mathematical trends, (b) Analytical modeling is safer and cheaper than the real engines testing, (c) Analytical modeling is efficient for design and development of engines since it works and gives insight into operations even before building the physical prototype of the engine answering the "what if" questions, (d) Analytical modeling gives insight beforehand into the expected problems and helps in fixing the unexpected problems, (e) Analytical modeling can speed up the design and development process of engines.

---

* Corresponding author
E-mail address: salah.elmoselhy@msm.nl

Frequency is critical to the design and performance analysis of combustion engines. Milašinović et al., [2] developed a semi-empirical method for evaluating the torsional vibration of a reciprocating engine. They determined the natural frequency from the harmonic analysis of the speed variation of the crankshaft's free end. The study then computationally evaluated the torsional stiffness coefficient of an equivalent mechanical system's crankshaft section. That study replaced the actual system with an equivalent system of a lumped parameter. The team of Milašinović found that the determination of the equivalent system's parameters is critical to the estimation of torsional stiffness and damping coefficients. The study further highlighted the difficulty of determining the torsional stiffness coefficient of the crankshaft, particularly due to the difficulty in capturing the real boundary conditions of operating the crankshaft. However, the work of Milašinović et al., [2] was developed based on a set of data. In addition, vehicle-to-vehicle correlation is impossible due to the variability between nominally identical vehicles. Thus, the model may need recalibration each time the model is used with a different set of data. Witek et al. [3], conducted numerical modal analysis of the crankshaft of diesel engine. The Finite Element Model (FEM) was constructed based on scanning a damaged crankshaft. The damaged crankshaft was scanned using Scanning Electron Microscope (SEM) [3]. In this modal analysis both the frequencies and modes of free vibration were obtained. That modal analysis showed that the main reason of premature failure is the resonant vibration of the crankshaft. However, that research lacks the merit of analytical modeling of the frequency of crankshaft. Kim and Lee [4] proposed an empirical model of the stiffness of the crankshaft. Kim and Lee [4] made tuning and adjustment of the preliminary model based on experimental measurements. However, their model does not analytically incorporate factors such as the brake thermal efficiency that indicates the overall efficiency of the system. Also, the work was developed based on a set of data. Thus, the model may need recalibration each time the model is used with a different set of data.

The frequency-related aspects such as natural frequency and stiffness of crankshaft are also related to the strain energy in the crankshaft. The elastic strain energy is a key approach to understanding the interplay between energy, mechanics of materials and failure phenomena. It is based on analyzing the strain energy stored in elastic members of a structure considering the various types of loading the structure is subjected to such as torsion and bending. Saxena and Ambikesh [5] utilized the elastic strain energy in deformable bodies for reducing the weight of engine components like connecting rod, crank shaft and piston. They thus developed a finite element model of the connecting rod for reducing the weight of the engine effectively and hence increasing the efficiency of the engine using the ANSYS software. The study further compared several alternatives of the structural material of the connecting rod using elastic strain energy for optimizing the structure. Bhise and Ramachandran [6] computationally modeled engine dynamics using a finite element method. Their computational model computed the equivalent inertia and stiffness of the crankshaft. For torque estimation, the paper based the model on the cylinder pressure as a key engine parameter with considerable potential for control applications. Yet, their dynamic model of a 4-cylinder diesel engine assumes a rigid crankshaft.

Stress concentration is another important pillar in the powertrains modeling. Witek et al. [3], also conducted numerical modal analysis of the crankshaft and showed that during the second mode of free vibration the high stress was concentrated in the zone of crack origin and the maximum stress area was located in the zone of crack origin. However, that work lacks the merit of the analytical modeling of the frequency of crankshaft. Fonte et al. [7], adopted an experimental approach using vibration analysis and the SEM analysis for investigating the failure mode of a diesel engine crankshaft. The research group of Fonte [7] reached the result that a crack at the crankpin web-fillet was the reason behind failure with a fatigue failure mechanism. In addition, the study reported the root cause of the crack as being   assembly misalignment of the crankshaft's main journal. However, that work did not adopt an analytical approach for modeling the frequency response of crankshaft. In addition, Kim and Lee [4] investigated the crankshaft's stress concentration. They inspected the concentrated stress at the crank pin fillet using rosette gauge positioned at 45° angle from the crankshaft's axis in the elevation view. That strain gauge enabled Kim and Lee [4] to evaluate the crankshaft's fatigue strength. The paper reported that the highly stressed area due to crankshaft's dynamics is found near the crankpin. Witeka et al. [8], used a nonlinear finite element method for determining the operational stress and thus analyzing failure on the crankshaft of diesel engine. The research team of Witeka [8] utilized the 3D optical scanner for scanning the surface discontinuities of a broken crankshaft for obtaining the geometry of the crankshaft as input to the finite element model. The obtained geometry was then exported to the ABAQUS-CAE pre-processor. The study concluded that the crack origin was found at the region of the maximum principal stress which was found at the discontinuity of interfacing the crank pin with the crank web. The study

also reported that the crack origin was not formed due to material defects or corrosion. The study also concluded that the premature fatigue failure was due to high-cycle fatigue in the zone of the crack in the crank pin. However, that work did not investigate the analytical modeling of the crankshaft's frequency. Giakoumis et al. [9], investigated both the steady-state and transient operations of turbocharged diesel engines and inspected the resulting crankshaft torsional deformation. The research group of Giakoumis analytically investigated the torque in the crankpin of crankshaft. The research work hence identified the underpinning mechanism of the torsional deformations in crankshafts. That research group related the torque to the rotational speed and used a case study for validating that model. That research group concluded that considerable deformation is expected depending on the engine-load configuration (load change & crankshaft stiffness). However, the model does not address the dynamics of crankshaft.

Sustainability in this field of automotive research is the capacity to maintain or improve the state and availability of desirable materials or conditions over the long term with respect to the environmental, economic and/or social aspects. Hence, the present paper is relevant to sustainability in the sense that the paper serves improving the state and availability of environmentally friendly diesel engines operations over the long term with respect to the environmental and economic aspects. Actually the homogeneity/stratification of the charge in homogeneous charge compression ignition (HCCI) engines is related to the stability of charging and stability of the engine [10]. The crankshaft's flexibility can affect the homogeneity/stratification of the charge in the homogeneous charge compression ignition (HCCI) engines. This is applicable to the proposed combustion system of hybrid Hydrogen-Biofuel charging, which was proposed in 2017 [11]. Thus, the present paper contributes to this research area.

Rakha et al. [12] highlighted that a widely valid and microscopic model of diesel engines is needed for evaluating diesel engines technologies. Faris et al., [13] thus modeled analytically the intake manifold of supercharged diesel engines, but without taking into consideration the flexibility of crankshaft. The flexibility of the crankshaft exhibits some nonlinearities to the dynamics of diesel engines, so that it can have impact on both the fuel consumption rate and the exhaust emissions rate [14]. Mei et al., [15] measured the exhaust CO, HC, and NOx emissions from light-duty vehicles under real driving conditions. The team of Mei analyzed the relationships between the emission characteristics of regulated gaseous pollutants and the operating conditions such as speed, acceleration, and specific power. They found that the road conditions had a significant impact on the regulated gaseous emissions, especially for HC emissions. Their paper reported that CO, NOx, and HC emissions in urban areas increase compared with those on highway roads.

Albeit the vehicular analytical modeling provides a physically explainable model, no model has as yet addressed the dynamics of crankshaft with respect to strain energy taking into account the crankshaft's flexibility. The present paper thus addresses this research gap. The key delivery of the present paper is to analytically model the strain energy-based aspects, frequency-related aspects and stress concentration in diesel engines whilst the flexibility of the crankshaft of engine is considered. In an endeavor to analyze and prevent materials failures in vehicular crankshafts, the present paper investigates the failure mechanisms, the identification of the failure's root causes, and the proposal of preventive actions to avoid failures. The present paper thus provides:(1) Failure analysis based on analytical modeling of crankshafts; (2) Investigation of failure mechanisms in crankshafts.

The present paper aims to provide the following contributions: (1) Modeling the strain energy in the flexible crankshaft (U_{Total}) analytically (section 3); (2) Simplifying the developed model for control applications based on the sensitivity analysis of the analytically modeled strain energy (section 4); (3) Validating the analytical modeling of the strain energy of the flexible crankshaft using case studies (section 5); (4) Proposing to remedy the stress concentration in the most critical section in crankshaft by identifying: (i) the location of the most critical section of stress concentration in crankshaft, (ii) the effect of the radius of the crankpin shoulder fillet on the maximum shearing stress and maximum bending stress that can be carried by the crankpin (section 6); (5) Facilitating the determination of the value of the radius of the crankpin shoulder fillet that remedies the stress concentration in the most critical section of stress concentration in crankshaft (section 6); (6) Analyzing how sensitive to the change in the independent variables the stress concentration factor for torsional load (K_t) and the stress concentration factor for bending load (K_b) are (section 7). A flowchart to visually represent the modelling process is shown in Figure 1.
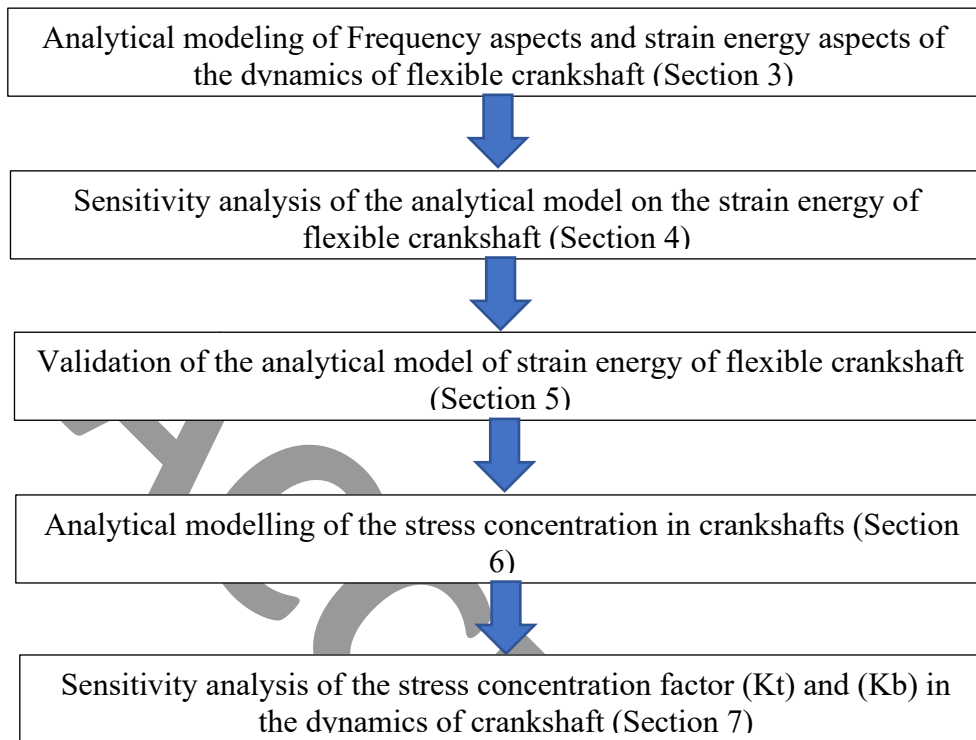
```
┌─────────────────────────────────────────────────────────────┐
│  Analytical modeling of Frequency aspects and strain energy  │
│  aspects of the dynamics of flexible crankshaft (Section 3)  │
└─────────────────────────────────────────────────────────────┘
                              ↓
┌─────────────────────────────────────────────────────────────┐
│  Sensitivity analysis of the analytical model on the strain  │
│  energy of flexible crankshaft (Section 4)                   │
└─────────────────────────────────────────────────────────────┘
                              ↓
┌─────────────────────────────────────────────────────────────┐
│  Validation of the analytical model of strain energy of      │
│  flexible crankshaft (Section 5)                             │
└─────────────────────────────────────────────────────────────┘
                              ↓
┌─────────────────────────────────────────────────────────────┐
│  Analytical modelling of the stress concentration in         │
│  crankshafts (Section 6)                                     │
└─────────────────────────────────────────────────────────────┘
                              ↓
┌─────────────────────────────────────────────────────────────┐
│  Sensitivity analysis of the stress concentration factor     │
│  (Kt) and (Kb) in the dynamics of crankshaft (Section 7)     │
└─────────────────────────────────────────────────────────────┘
```

Figure 1. Flowchart to visually represent the modelling process.

2 Materials and methods

The present research work is quantitative and is based on a theoretical approach employing exploratory and computational techniques. Analytical modeling, which is widely valid, is employed in the present research. Analytical models are developed in this research for rationally providing explainable and self-validated models. The present study analytically modeled: (i) the strain energy in the flexible crankshaft in engines, (ii) the effect of the radius of the crankpin shoulder fillet on the maximum shearing stress and maximum bending stress that can be carried by the crankpin, (iii) the radius of the crankpin shoulder fillet that remedies the stress concentration in the most critical section of stress concentration in crankshaft. Case studies for validating the developed analytical models are employed in the present research as well. The finite element modeling and analysis have been adopted in some of these case studies.

The finite element analysis (FEA) which is presented in section "6" in the present paper, was not conducted by the authors, as stated in section "6" such as in Table 4 highlighting that the FEA was based on case studies. These case studies listed in Table 4 in section "6" prove the validity and viability of the proposed idea and deduction in section "6". Actually, from the research methodology perspective, having the FEA conducted by other researchers as case studies further robustly and credibly proves the proposed idea and deduction in the present paper, since no potential bias can exist in these FEAs, because those reference papers of case studies are not written by the authors.

For simplifying the analytical models on the dynamics of the alloy steel crankshaft of diesel engines, the sensitivity analysis is utilized. The sensitivity analysis is employed to show: (1) how sensitive the strain energy in the flexible crankshaft is to its independent variables, (2) how sensitive the stress concentration factor is to the changes in its independent variables. The mechanical properties of the alloy steel crankshaft of the diesel engine include [3, 7]: (a) the modulus of elasticity is 200 GPa, (b) the shear modulus 78 GPa, (c) the yield strength is 480 MPa.

The present study is not addressing the transient response in the diesel engine, but rather the steady state performance thereof. The steady state requires that the condition and properties of all points in the system

remain unchanging with respect to time. Actually the present paper adopts the class of "mean value model" in engine modeling. Therefore, the representative average value is basically adopted in the present paper. There are several research papers that adopt this class of modeling, i.e. the "mean value model", such as [16, 17].

From the conservative perspective, the assumptions in the present research include: (a) creep failure based on time-varying loading and temperature varying loading is not considered; (b) standard deviation in the average values used for validating the developed analytical models is small, and thus can be negligible; (c) all vehicles consume fuel and pollute similarly for the same distance and at the same speed [18]; (d) all vehicles operate on the highways at constant speed [19]; (e) driver's behavior is invariable [20]; (f) the difference in altitude in the engine is negligible; (g) considering the control volume in the engine, the fluid flow is quasi 1-Dimensional flow; (h) the density of the fuel in the engine is constant [21]; (i) no change in phase in the air flow, so that air is an ideal gas [22]; (j) the mass of the working fluid is conserved [22]; (k) volumetric efficiency is assumed to be constant [23]; (l) the investigated load case is quasi-static.

3   Frequency aspects and strain energy aspects of the dynamics of flexible crankshaft

Torsional vibration is more often than not a key concern in power transmission systems using crankshafts where it can cause failure if not designed and controlled properly. This is particularly true when the frequency of the torsional vibration of the crankshaft resonates with the natural frequency of the crankshaft system. In internal combustion engines, torsional vibration emerges from a couple of causes: (i) non-smoothness of the torque generated by the cylinders of the engine, (ii) eccentricity due to wear, fabrication defects, and/or misalignment. The first cause is often tackled by proper configuration of the geometric alignment/positioning of the cylinders of the engine, proper firing order of the cylinders of the engine, and attaching a flywheel to one end of the crankshaft. The second cause is often tackled by forging in the manufacturing process for getting rid of micro-structural porosities and then by adding counter-weights. In addition, the second cause is analytically modeled in this section of the present paper.

Engines with six or more cylinders in a straight line configuration render the crankshaft's flexibility more noticeable, due to its relatively long length. The two-stroke engine often provides higher power than the four-stroke engine counterpart, so that the decreased stiffness and increased flexibility of the crankshaft could become then nontrivial. Figure 2 shows the real crankshaft from an isometric perspective, so that it gives insight into the construction parameters and specifications of the crankshaft and how the crankshaft looks like in the real world. A typical crankshaft as shown in Figure 2 contains five centrally-located coaxial cylindrical ("main") journals and four offset cylindrical crankpins ("rod") journals, each spaced 180° from its neighbors.

The sources of forces applied onto a crankshaft are: (i) the combustion chamber pressure acting on the piston, (ii) the centrifugal force due to offset of the weights rotating with the crankshafts, (iii) the weights of the crankshaft and its attachments, (iv) the force dissipated in the acceleration of the mass of the piston. Compression-Ignition (CI) engines can generate combustion pressures in the 200-bar neighborhood.

Because the secondary piston acceleration forces are parallel with the cylinder axes, in this engine design analysis the vertical components of those forces on a given crankpin cancel each other. The horizontal components of the piston acceleration forces can have influence on the friction loss of the piston . However, the horizontal components of the piston acceleration forces are often small enough to be neglected, given the small mass of the piston, less than 1 kg [24].

Figure 2. 4-Cylinder-basedcrankshaft for Isuzu NPR truck 4HG1 diesel engine.

The mass flow rate of the air that goes into all the cylinders of the engine, $\dot{m}_{AC}$, can be affected by the flexibility of the crankshaft that is a function of the velocity of the piston which is a function of the crank's geometry. The condition of flexibility is mainly:

$$\omega_c \geq \omega_n \tag{1}$$

where: ω_c crankshaft's operating rotational speed (Hz); ω_n crankshaft's natural frequency (Hz). Only in the theoretically extreme case, the equality is included. Actually, the extreme value of the working frequency can reach the value of the natural frequency in such a case of resonance. Following from the definition of the natural frequency of the crankshaft, ω_n, equation (1) can be rewritten as follows:

$$\omega_c \geq \sqrt{\frac{K_c}{m_c}} \tag{2}$$

where: K_c is the stiffness of the crankshaft (N/m); m_c is the mass of the crankshaft and its connected components such as pistons and connecting rods (kg).

The operating rotational speed (ω_c) influences the imposed force onto the crankshaft. The total force exerted by the crankshaft (F_{Total}) and indicated in Figure 3, can be analytically formulated as follows:

$$F_{Total} = \eta_{bt} \sqrt{F_t^2 + F_r^2} \tag{3}$$

where: η_{bt} is the brake thermal efficiency of the engine, which is a measure of the overall efficiency of the engine, representing the ratio of energy in the brake power to the fuel energy and taking into account the inefficiency in the cycle and the process; F_t is the tangential component of the total force exerted by the crankshaft (N), as indicated in Figure 3; F_r is the radial component of the total force exerted by the crankshaft (N), as indicated in Figure 3. A side view of the crankshaft and the connecting rod assembly is shown in Figure 4.
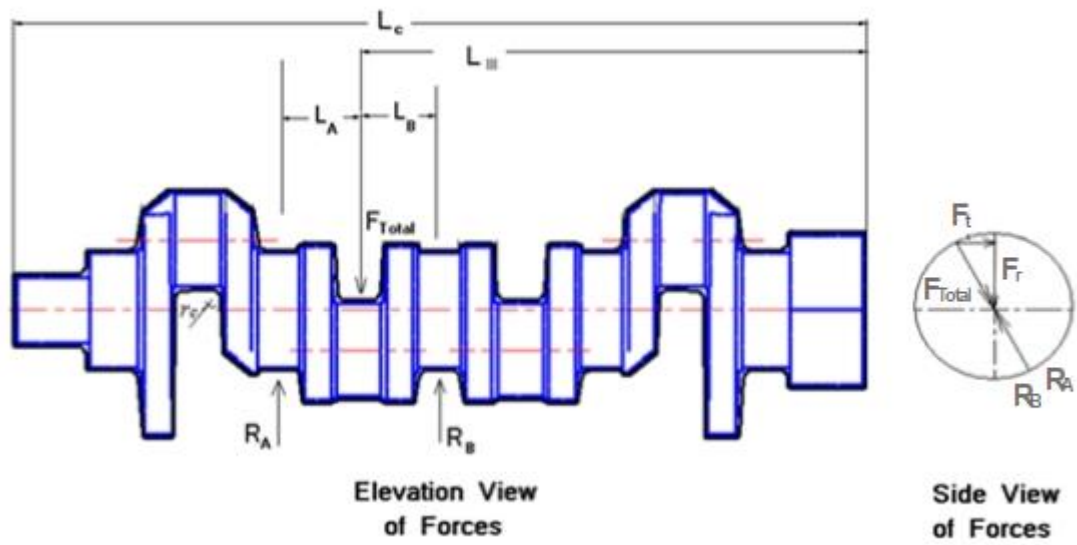
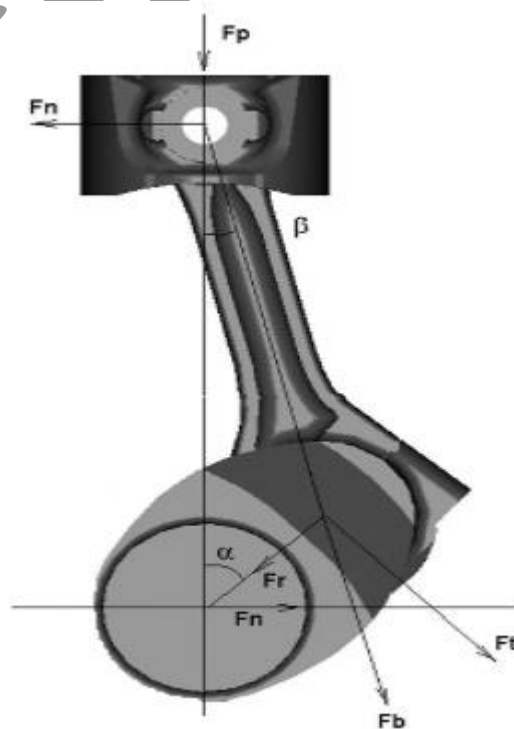Figure 3. Schematic diagram of the forces exerted onto the 2nd crank of a diesel 4-cylinder engine.

Figure 4. Side view of the crankshaft and the connecting rod assembly in diesel engine.

As can be gathered geometrically from Figure 4, the tangential component of the total force (F_t) is:

$$F_t = F_{tP} - F_{tI} - F_{tE} + F_{tW} \tag{4}$$

where: F_{tP} is the tangential force due to the pressure in the cylinder (N); F_{tI} is the tangential force due to inertia (N); F_{tE} is the tangential force due to eccentricity (N); F_{tW} is the tangential component of the weight of crankshaft (N). Inertia is the object's tendency to remain in its static or motional state, so that it is the resistance

to acceleration and is proportional to the mass of the object. Firstly, the tangential force due to the pressure in the cylinder, F_{tP}, can be analytically modeled based on Figure 4 as:

$$F_{tP} = N_{Cyl} \; P_{Cyl} \; \frac{\pi \; D_{Cyl}^2}{4} \; \frac{sin(\alpha + \beta)}{cos(\beta)} \tag{5}$$

where: N_{Cyl} is the engine's number of the cylinders; P_{Cyl} is the pressure inside each of the cylinders of the engine (N/m²); D_{Cyl} is the diameter of each of the cylinders of the engine (m); α is the crank angle, as indicated in Figure 4; β is the connecting rod's angle of rotation, as indicated in Figure 4. The angle of rotation of the connecting rod of the engine, β, can be analytically formulated based on Figure 4 as follows:

$$\beta = sin^{-1}\left(\frac{R_{crank}}{L_{conrod}} \; sin(\alpha)\right) \tag{6}$$

where: L_{conrod} is the length of the connecting rod (m); R_{crank} is the radius of the crank (m).

The pressure inside each of the cylinders of the engine, P_{Cyl}, can be analytically modeled as the mean effective pressure inside the cylinder [25]:

$$P_{Cyl} = \frac{T_{max}}{\frac{\pi}{4} \; D_b^2 \; R_{crank} \; sin(\alpha) \; \left(1 + \frac{R_{crank}}{L_{conrod}} \; cos(\alpha)\right)} \tag{7}$$

where: D_b is the bore diameter; T_{max} is the engine's brake maximum torque (N.m). Secondly, the tangential force due to inertia, F_{tI}, can be analytically modeled based on Figure 4, as:

$$F_{tI} = N_{Cyl} \left(\frac{m_R}{3}\right) R_{crank} \; \omega_c^2 \left[cos(\alpha) + \left(\left(\frac{R_{crank}}{L_{conrod}} \; cos(2\,\alpha)\right)\right)\right] \frac{sin(\alpha + \beta)}{cos(\beta)} \tag{8}$$

where: m_R is collectively the masses associated with the crank under consideration (kg). Thirdly, the tangential force due to eccentricity, F_{tE}, can be analytically modeled as:

$$F_{tE} = N_{Cyl} \left(\frac{m_R}{3}\right) \omega_c^2 \; e_c \; cos(\omega_c \, t) \tag{9}$$

where: e_c is the eccentricity in the crank of the crankshaft from its geometric centre due to the masses associated with the crankshaft, which relatively indicates the flexibility of the crankshaft (m); t is time (s). Fourthly, the tangential component of the weight of crankshaft, F_{tW}, can be analytically modeled as:

$$F_{tW} = \; m_c \; g \; sin(\alpha) \tag{10}$$

where: g is the gravitational acceleration. Similarly, as can be gathered geometrically from Figure 4, the radial component of the total force (F_r) is:

$$F_r = \; F_{rP} - \; F_{rI} - \; F_{rE} + \; F_{rW} \tag{11}$$

where: F_{rP} is the radial force due to the pressure in the cylinder (N); F_{rI} is the radial force due to inertia (N); F_{rE} is the radial force due to eccentricity (N); F_{rW} is the radial component of the weight of crankshaft (N). Thus, the radial force due to the pressure in the cylinder, F_{rP}, can be analytically modeled based on Figure 4, as:

$$F_{rP} = N_{Cyl} \, P_{Cyl} \, \frac{\pi \, D_{Cyl}^2}{4} \, \frac{cos \, (\alpha \, + \, \beta)}{cos(\beta)} \tag{12}$$

Also, the radial force due to inertia, F_{rI}, can be analytically modeled based on Figure 4 as:

$$F_{rI} = N_{Cyl} \left(\frac{2 \, m_R}{3}\right) R_{crank} \, \omega_c^2 \left[cos(\alpha) + \left(\left(\frac{R_{crank}}{L_{conrod}} \, cos(2 \, \alpha)\right)\right)\right] \frac{cos(\alpha \, + \, \beta)}{cos(\beta)} \tag{13}$$

Moreover, the radial force due to eccentricity, F_{rE}, can be analytically modeled as:

$$F_{rE} = N_{Cyl} \left(\frac{2 \, m_R}{3}\right) \, \omega_c^2 \, e_c \, sin(\omega_c \, t) \tag{14}$$

Also, the radial component of the weight of crankshaft, F_{rW}, can be analytically modeled as:

$$F_{rW} = \, m_c \, g \, cos(\alpha) \tag{15}$$

Hence, following from equations (3), (4) and (11), the total force exerted by the crankshaft (F_{Total}) can be analytically formulated as follows:

$$F_{Total} = \, \eta_{bt} \, \sqrt{[\, F_{tP} - \, F_{tI} - \, F_{tE} + \, F_{tW}]^2 + [F_{rP} - \, F_{rI} - \, F_{rE} + \, F_{rW}]^2} \tag{16}$$

As can be gathered from Figure 3, the crank and its two journal bearings mounted on the shaft can be generically modeled as a simply supported beam subjected to F_{Total} with a reaction at each of the two bearings A and B. Thus, from the equilibrium of forces on this simply supported beam:

$$F_{Total} = \, R_A + \, R_B \tag{17}$$

Static equilibrium is achieved when the sum of all forces acting on an object is zero, and the sum of all torques acting on the object is zero. Dynamic equilibrium is achieved when the sum of all torques acting on the object is equal to the product of the mass moment of inertia I_c times the angular acceleration $\ddot{\alpha}_c$. The mass moment of inertia is a property of an object that quantifies its resistance to changes in rotational motion around an axis of rotation. Dynamic equilibrium indicates continuous change in the object's motion. In the steady state of the crankshaft, the equilibrium is quasi-static. Actually the average expansion angular crankshaft acceleration of the crankshaft $\ddot{\alpha}_c$ is 233 rad/s^2 [26]. Also, the average mass moment of inertia of the crankshaft I_c is 0.0015 kg.m^2 [27]. Thus, the product of I_c times $\ddot{\alpha}_c$ is about 0.3 N.m, which is very small value that is very close to zero, depicting the quasi-static equilibrium in steady state. Therefore, from the equilibrium of moments on this simply supported beam:

$$\sum M_B = I_c \, \ddot{\alpha}_c \, , \quad F_{Total}(L_B) - \, R_A \, (L_A \, + \, L_B) = I_c \, \ddot{\alpha}_c \tag{18}$$

Hence, from equations (18) and (16):

$$R_A = \eta_{bt} \frac{L_B}{L_A + L_B} \sqrt{[F_{tP} - F_{tI} - F_{tE} + F_{tW}]^2 + [F_{rP} - F_{rI} - F_{rE} + F_{rW}]^2} \tag{19}$$

Substituting equation (19) into equation (17):

$$R_B = \eta_{bt} \left(1 - \frac{L_B}{L_A + L_B}\right) \sqrt{[F_{tP} - F_{tI} - F_{tE} + F_{tW}]^2 + [F_{rP} - F_{rI} - F_{rE} + F_{rW}]^2} \tag{20}$$

Since the crankshaft is subject to bending moment and torsion, the total strain energy of the crankshaft within the elastic range of loading (U_{Total}) can now be analytically modeled using the principles of superposition and conservation of energy:

$$U_{Total} = U_{Bending} + U_{Torsion} \tag{21}$$

where: $U_{Bending}$ is the strain energy of the crankshaft due to bending moment (J); $U_{Torsion}$ is the strain energy of the crankshaft due to torsion (J). Thus:

$$U_{Total} = \left[\frac{1}{2E_c I_c}\int_0^{L_A}(R_A x)^2 dx\right] + \left[\frac{1}{2E_c I_c}\int_0^{L_B}(R_B x)^2 dx\right] + \left[\frac{\left(\frac{T_{\max}}{N_{Cyl}}\right)^2 (L_A + L_B)}{2G_c J_c^2}\right] \tag{22}$$

where: E_c is the modulus of elasticity of the material of the crankshaft (N/m^2); I_c is the mass moment of inertia of the crankshaft (kg.m^2); G_c is modulus of rigidity of the material of the crankshaft (N/m^2); J_c is the polar moment of inertia (kg.m^2). Hence, the total strain energy of the crankshaft (U_{Total}) can now be analytically formulated following from equation (22) as follows:

$$U_{Total} = \left[\frac{R_A^2 L_A^3}{6E_c I_c}\right] + \left[\frac{R_B^2 L_B^3}{6E_c I_c}\right] + \left[\frac{\left(\frac{T_{\max}}{N_{Cyl}}\right)^2 (L_A + L_B)}{2G_c J_c^2}\right] \tag{23}$$

This analytical formulation of the U_{Total} can help in analyzing the modes of structural failure in crankshafts. The following section investigates the simplification of the U_{Total} analytical model using the sensitivity analysis.

4 Sensitivity analysis on the strain energy of flexible crankshaft

For enabling efficient use of the U_{Total} model, i.e. equation (23), it is simplified through the analysis of its sensitivity to the change in independent variables. The sensitivity analysis is based on applying the sensitivity ratio, $R_{Sensitivity}$, formulation to each of the independent variables. While evaluating $R_{Sensitivity}$ for each independent variable, the values of the remaining independent variables remain unchanged from the baseline values. This $R_{Sensitivity}$ is formulated as follows [28]:

$$R_{Sensitivity} = \frac{\dfrac{V_{Dependent\,Changes} - V_{Dependent\,Baseline}}{V_{Dependent\,Baseline}}}{\dfrac{V_{Independent\,Changes} - V_{Independent\,Baseline}}{V_{Independent\,Baseline}}} \tag{24}$$

where: $V_{DependentChanges}$ is the value of the dependent variable in the analytical model with the increment/decrement of change; $V_{DependentBaseline}$ is the baseline value of the dependent variable in the analytical model; $V_{IndependentChanges}$ is the value of the independent variable in the analytical model with the increment/decrement of change; $V_{IndependentBaseline}$ is the baseline value of the independent variable in the analytical model. The key explanatory variable in this model is the mass moment of inertia of the crankshaft (Ic). The baseline value of the Ic is "1.5×10^{-3} kg.m^2", which is proportional with the engine power as in [27]. The sensitivity analysis on U_{Total} is detailed in Table 1 based on equations (23) and (24).

Table 1. Sensitivity analysis on the U_{Total}.

	-50% Decrement Below Baseline Value	-25% Decrement Below Baseline Value	Baseline Value	+25% Increment Above Baseline Value	+50% Increment Above Baseline Value	Average Sensitivity Ratio on Each Independent Variable
U_{Total}	1.25×10^{-5}	1.875×10^{-5}	2.5×10^{-5}	3.125×10^{-5}	3.75×10^{-5}	N/A
E_c	100 GPa	150 GPa	200 GPa [6]	250 GPa	300 GPa	N/A
$R_{Sensitivity}$, on E_c	1	1	N/A	1	1	1
U_{Total}	1.25×10^{-5}	1.875×10^{-5}	2.5×10^{-5}	3.125×10^{-5}	3.75×10^{-5}	N/A
L_A	0.057 m	0.085 m	0.1130 m [29]	0.141 m	0.169 m	N/A
$R_{Sensitivity}$, on L_A	1	1	N/A	1	1	1
U_{Total}	1.25×10^{-5}	1.875×10^{-5}	2.5×10^{-5}	3.125×10^{-5}	3.75×10^{-5}	N/A
R_{crank}	0.0362 m	0.0543 m	0.0725 m [2]	0.0906 m	0.1087 m	N/A
$R_{Sensitivity}$, on R_{crank}	1	1	N/A	1	1	1
U_{Total}	1.25×10^{-5}	1.875×10^{-5}	2.5×10^{-5}	3.125×10^{-5}	3.75×10^{-5}	N/A
η_{bt}	0.175	0.262	0.35 [30]	0.437	0.525	N/A
$R_{Sensitivity}$, on η_{bt}	1	1	N/A	1	1	1
U_{Total}	1.25×10^{-5}	1.875×10^{-5}	2.5×10^{-5}	3.125×10^{-5}	3.75×10^{-5}	N/A

T_{max}	93 N.m	139.5 N.m	186 N.m [3]	232.5 N.m	279 N.m	N/A
$R_{Sensitivity,}$ on T_{max}	1	1	N/A	1	1	1
U_{Total}	1.25×10^{-5}	1.875×10^{-5}	2.5×10^{-5}	3.125×10^{-5}	3.75×10^{-5}	N/A
Gc	39 GPa	58 GPa	78 GPa [6]	97 GPa	117 GPa	N/A
$R_{Sensitivity,}$ on Gc	1	0.975	N/A	1.03	1	1
U_{Total}	1.25×10^{-5}	1.875×10^{-5}	2.5×10^{-5}	3.125×10^{-5}	3.75×10^{-5}	N/A
Jc	0.05 kg.m^2	0.075 kg.m^2	0.1 kg.m^2 [2]	0.125 kg.m^2	0.15 kg.m^2	N/A
$R_{Sensitivity,}$ on Jc	1	1	N/A	1	1	1
U_{Total}	1.25×10^{-5}	1.875×10^{-5}	2.5×10^{-5}	3.125×10^{-5}	3.75×10^{-5}	N/A
Ic	0.75×10^{-3} kg.m^2	1.125×10^{-3} kg.m^2	1.5×10^{-3} kg.m^2 [27]	1.875×10^{-3} kg.m^2	2.25×10^{-3} kg.m^2	N/A
$R_{Sensitivity,}$ on Ic	1	1	N/A	1	1	1

The U_{Total} is hence sensitive to the change in E_c, L_A, L_B, R_{crank}, η_{bt}, T_{max}, Gc, Jc, and Ic. Hence, E_c, L_A, L_B, R_{crank}, η_{bt}, T_{max}, Gc, Jc, and Ic in equation (23) should not be considered a constant. Thus, the sensitivity analysis cannot provide a simpler form of the U_{Total} model, i.e. equation (23). The U_{Total} model is validated in the following section.

5   Validation of the analytical model of strain energy of flexible crankshaft

The validation of the analytical model of the U_{Total} that has been developed in equation (23) is investigated in this section. The validation is conducted through case studies and the results are analyzed statistically. The collected data are based on a couple of case studies extracted from the literature. This approach is meritorious in several senses including to eliminate the possibility of having bias in the measured data. A case study has been conducted utilizing a four-cylinder diesel engine S-4003 with Swept Volume of 3120 cm^3 that provides maximum power of 33 kW at about 2000 rpm [3, 31]. The field data represent an operating point at the rotational speed of 2000 rpm [3, 2] and brake thermal efficiency of 35 % [32] are shown in Table 2. For the diesel engine S-4003, the compression ratio of (17:1) is used [31]. The rotational speed of 2000 rpm is an average speed of the engine [31]. This value of efficiency can be justified in light of the fact that the efficiency of the internal combustion engine drops once it propels a vehicle, since a significant portion of the total power is emitted as heat loss without being turned into useful work. Some of the total power generated is also lost as friction, air turbulence, and work used to turn engine related equipment such as water and oil pumps [30]. Therefore, reducing frictional losses is a key aim in the design of engines for increasing the efficiency and reducing tribological wear [33-35]. The crankshaft's angle of rotation, (α) in Figure 4, is 370 degrees in the power stroke, at which the peak pressure is reached in the cylinder of the engine [36].

Table 2. Field data of a case study implemented on the strain energy of flexible crankshaft [U$_{Total}$].

Parameter	Value extracted from field data	Reference
U$_{Total}$	2.5 x 10^{-5}	[5, 6]
N$_{Cyl}$	4	[3]
P$_W$	38.8 kW	[3]
T$_{max}$	186 N.m	[3, 31, 37]
R$_{crank}$	0.072 m	[2]
m$_R$	2.15 kg	[38]
ω$_c$	2000 rpm	[3]
e$_c$	0.08 x 10^{-3} m	[29]
α (i.e. ω$_c$ t)	370 degree (in the power stroke)	[36]
m$_c$	7.5 kg	[27]
L$_A$ (for L$_c$ of 0.9 m)	0.113 m	[29]
L$_B$ (for L$_c$ of 0.9 m)	0.113 m	[29]
L$_c$	0.90 m	[29]
E$_c$	200 GPa	[3, 6, 7]
I$_c$	1.5* 10^{-3} kg.m^2	[27]
G$_c$	78 GPa	[3, 4, 7]
J$_c$ (proportional to the engine power)	0.1 kg.m^2	[2]

For having R$_A$ of equation (19) representing half of the total force exerted by the crankshaft, *F$_{Total}$*, based on symmetry the corresponding value of the L$_A$ would be proportionally half of the L$_C$. Based on Equation (23) and Table 2, the strain energy of flexible crankshaft (*U$_{Total}$*) is 2.7 x 10^{-5}. The relative error of the model, ε_R , is the statistical measure in the present study. The ε_R is evaluated as follows [39]:

$$\varepsilon_R = \sum_{i=1}^{z_n} \left| \frac{y_i - x_i}{y_i} \right| \frac{100\%}{z_n} \tag{25}$$

where: x$_i$ is the interval variable which is the analytically expected value; y$_i$ is the interval variable that is the measured value, i.e., field dataset; z$_n$ is the number of records in the sample. The ε_R is a quantifiable measure

of statistical validation. The data of this case study is statistically analyzed in Table 3 following from equation (25).

Table 3. Summary of statistical analysis on U_{Total}.

Table #	$\bar{x}$	$\bar{y}$	ε_{R}
Table 2	2.7 x 10^{-5}	2.5 x 10^{-5}	*8%*

This analytical formulation of the U_{Total} that is often associated with the modes of structural failure in mechanics of materials paves the way for investigating the analytical modeling of the stress concentration in crankshafts.

6   Remedying the stress concentration in the most critical section of stress concentration in crankshaft

In-cylinder pressure is the key load that results in failure. What influences such a significant load in diesel engines was studied before [13]. The present paper addresses in this section the cause of such failure and how to remedy that failure. Normally the dynamic loading imposed onto the crankshaft results in significant stress concentration that can eventually result in fracture. A finite element analysis has been conducted on the maximum principal stress distribution for the crankshaft of a 4-stroke 4-cylinder diesel engine during free vibration at resonant frequency (Frequency 2000 Hz), as shown in Figure 5. This approach is often used, such as under multi-axial loading [36].

Based on the finite element analysis and case studies, the expected location of crank origin due to stress concentration in flexible crankshafts is at the discontinuity interface between the crankpin and counterweight web as shown in Figure 5. Figure 5 shows the result of the finite element analysis of one of these case studies, i.e. reference [3]. Table 4 shows the case studies on the most critical section of stress concentration in crankshaft.

Contour Plot

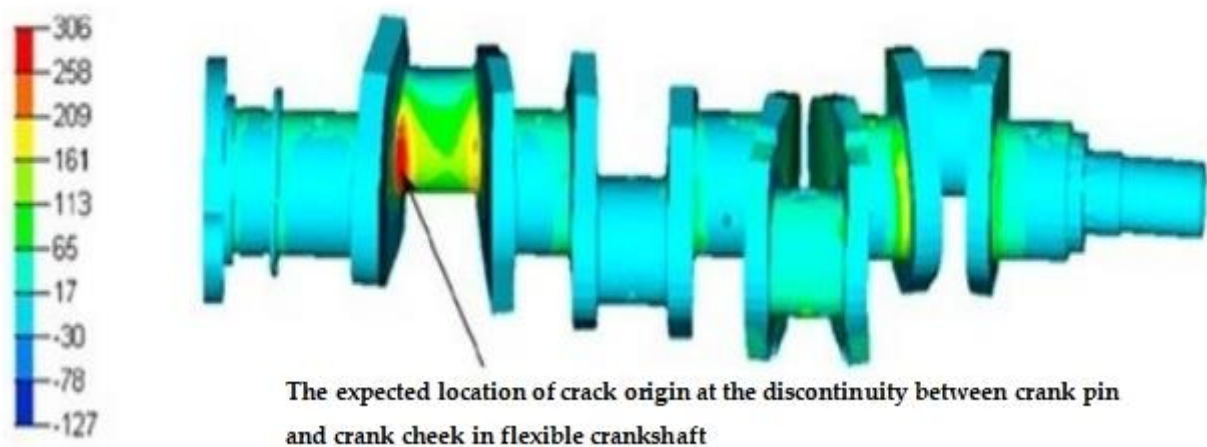**S-Stress Component (Max Principal)**

Maximum Average (MPa)

Figure 5. Maximum average principal stress distribution for the crankshaft of 4-stroke 4-cylinder diesel engine during free vibration at resonant frequency [Resonant frequency 2000 Hz].

Table 4. Case studies on the most critical section of stress concentration in crankshaft.

Engine Specification	Location of the Most Critical Section of Stress Concentration in Crankshaft	Reference
S-4003 4-cylinder diesel engine, Displacement is 3120 cm3, Maximum power is 33.12 kW at rotational speed of 2000 rpm	At the discontinuity interface between the crankpin and counterweight web	[3]
2.0 Liter DTI 4-cylinder diesel engine	At the discontinuity interface between the crankpin and counterweight web	[8]
Four-cylinder, four-stroke, diesel engine with power of 110 kW	At the discontinuity interface between the crankpin and counterweight web	[7]

The peak of stress concentration at the most critical section in the crankshaft is 306 MPa, which is less than the yield strength of the alloy steel crankshaft which is 480 MPa. Thus, no plasticity is detected at the critical section in the crankshaft.

The simultaneous effect of the radius of the crankpin shoulder fillet (r_c) on the maximum shearing stress that can be carried by the crankpin (τ_{ave}) and on the maximum bending stress that can be carried by the crankpin (M_{ave}) appears through the stress concentration factor of (K_t). The stress concentration factor of K_t depends on the ratio of the large and small diameters of the stepped shaft transmitting the torque (D_c and d_c, respectively) and on the ratio of the radius of the crankpin shoulder fillet (r_c) to the diameter of the smaller shaft which is the crankpin (d_c). These diameters (D_c and d_c) and the radius of the crankpin shoulder fillet (r_c) are shown below in the Figure 6.
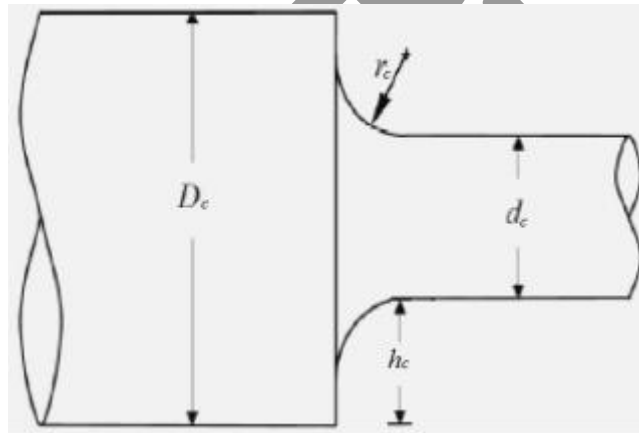

Figure 6. Stepped crankshaft transmitting torque through the crankpin and subjected to stress concentration

As to the effect of the radius of the crankpin shoulder fillet (r_c) on the maximum shearing stress that can be carried by the crankpin (τ_{ave}), the stress concentration in the crankshaft is proportional to the torque applied onto the crankshaft (T_{max}) through the crankpin that manifests a stepped shaft [40]:

$$\tau_{yield} = K_t\,\tau_{ave} \tag{26}$$

where: τ_{yield} is the torsional yield strength of the material of the crankshaft (N/m^2); K_t is the stress concentration factor; τ_{ave} is the maximum shearing stress that can be carried by the crankpin (N/m^2). The maximum shearing stress that can be carried by the crankpin is analytically formulated as [40]:

$$\tau_{ave} = \frac{16\,T_{max}}{\pi\,d_c{}^3} \tag{27}$$

where: d_c is the diameter of the crankpin (m). Thus:

$$\tau_{yield} = K_t\,\frac{16\,T_{max}}{\pi\,d_c{}^3} \tag{28}$$

The mathematical formulation of the stress concentration factor for the torsional load (K_t) for the shoulder fillet in crankshaft is [41]:

$$
\begin{aligned}
K_t = {}& \left[0.905 + 0.783\,\sqrt{\frac{h_C}{r_C}} - 0.075\,\frac{h_C}{r_C} \right] \\
& + \left[-0.437 - 1.969\,\sqrt{\frac{h_C}{r_C}} + 0.553\,\frac{h_C}{r_C} \right] \left(2\,\frac{h_c}{D_c} \right) \\
& + \left[1.557 + 1.073\,\sqrt{\frac{h_C}{r_C}} - 0.578\,\frac{h_C}{r_C} \right] \left(2\,\frac{h_c}{D_c} \right)^2 \\
& + \left[-1.061 + 0.71\,\sqrt{\frac{h_C}{r_C}} + 0.086\,\frac{h_C}{r_C} \right] (2\,h_c/D_c)^3
\end{aligned}
\tag{29}
$$

Similarly, for the effect of the radius of the crankpin shoulder fillet (r_c) on the maximum bending stress that can be carried by the crankpin (M_{ave}), the stress concentration in the crankshaft is proportional to the bending force applied onto the crankshaft (F_c) through the crankpin that manifests a stepped shaft [40]:

$$M_{yield} = K_b\,M_{ave} \tag{30}$$

where: M_{yield} is the bending yield strength of the material of the crankshaft (N/m^2); K_b is the stress concentration factor for the bending load; M_{ave} is the maximum bending stress that can be carried by the crankpin (N/m^2). The maximum bending stress that can be carried by the crankpin is analytically formulated as [40]:

$$M_{ave} = \frac{32\,M_{max}}{\pi\,d_c{}^3} \tag{31}$$

Thus:

$$M_{yield} = K_b\,\frac{32\,M_{max}}{\pi\,d_c{}^3} \tag{32}$$

The mathematical formulation of the stress concentration factor for the bending load (K_b) for the shoulder fillet in crankshaft is [41]:

$$K_b = \left[0.947 + 1.206\sqrt{\frac{h_c}{r_c}} - 0.131\,\frac{h_c}{r_c}\right] + \left[0.022 - 3.405\sqrt{\frac{h_c}{r_c}} + 0.915\,\frac{h_c}{r_c}\right]\left(2\frac{h_c}{D_c}\right)$$

$$+ \left[0.869 + 1.777\sqrt{\frac{h_c}{r_c}} - 0.555\,\frac{h_c}{r_c}\right]\left(2\frac{h_c}{D_c}\right)^2 \tag{33}$$

$$+ \left[-0.810 + 0.442\sqrt{\frac{h_c}{r_c}} - 0.260\,\frac{h_c}{r_c}\right](2\,h_c/D_c)^3$$

Hence, in the design of crankshafts, it is recommended to reduce K_t and K_b respectively in order to: (i) increase τ_{ave} and thus the maximum torque that can be transmitted by the crankpin, (ii) increase M_{ave} and thus the maximum bending force that can be withstood by the crankpin. Following from equation (29) for the torsional load on the crankpin, it is recommended to reduce the ratio of $[h_c/r_c]$ for minimizing K_t. However, following from equation (33) for the bending load on the crankpin, it is recommended to increase the ratio of $[h_c/r_c]$ for minimizing K_b.

Therefore, following from equations (29) and (33), it is recommended to conduct optimization of multi-objective functions based on equations (29) and (33) for determining the value of r_c that minimizes K_t and K_b given the geometrical input values of the D_c and h_c of the given specific design of crankshaft for a specific engine. It is also hence economically recommended to minimize the value of $[D_c–2h_c]$ whilst having the ratio of $[r_c/(D_c–2h_c)]$ as large as 0.3 for avoiding cracks at the crank cheeks. This value of 0.3 is taken as a benchmark here, since this is the usually attainable limit of the ratio of $[r_c/(D_c–2h_c)]$ for minimizing K_t [41]. The analytical formulation of the Stress Concentration Factor (K_t) can be simplified using the sensitivity analysis. The following section investigates the simplification of the K_t and K_b analytical models using the sensitivity analysis.

7   Sensitivity analysis of the stress concentration factor (K_t) and (K_b) in the dynamics of crankshaft

This section investigates how sensitive the developed model of the K_t and K_b is to the change in its independent variables. This analysis enables simplifying the analytical model. The sensitivity analysis relies on applying the sensitivity ratio, $R_{Sensitivity}$, formulation to each of the independent variables, as indicated in equation (24). The Stress Concentration Factor, K_t, is analytically modeled in equation (29) for the torsional load on the crankpin. Similarly the K_b is analytically modeled in equation (33) for the bending load on the crankpin. The key explanatory variable in this model is the ratio of the independent variables of the stepping shoulder height, h_c, to the radius of the crankpin shoulder fillet, r_c. In order to figure out the baseline value of the ratio of (h_c/r_c), some deductions would be made from the analytical models and some extractions would be made from the available databases. Following from Figure 6, we can deduce that $h_c = (D_c\text{-}d_c)/2$. For the crankshaft of the diesel engine of four-cylinder diesel engine S-4003 that is presented in the case study of section 5, D_c = 2.36 in (i.e. 0.0599 m) and d_c = 2.05 in (i.e. 0.0530 m) [42, 43]. Hence, h_c is 0.00347 m and the ratio (D_c/d_c) is 1.13. Following from the operational values of the ratio (r_c/d_c), for the ratio (r_c/d_c) of 0.05, the K_t is 1.28 and the K_b is 1.9 [44]. Therefore, the r_c is 0.0026 m and the ratio (h_c/D_c) is 0.0579. Hence, the baseline value of the ratio of (h_c/r_c) is (1.335). The sensitivity of the model of the K_t is analyzed in Table 5 utilizing equations (29), (33) and (24).

Table 5. Sensitivity analysis of the developed model of the K_t and K_b.

	-50% Decrement Below Baseline Value	-25% Decrement Below Baseline Value	Baseline Value	+25% Increment Above Baseline Value	+50% Increment Above Baseline Value	Average Sensitivity Ratio on Each Independent Variable
K_t (Torsion)	0.64	0.96	1.28	1.6	1.92	N/A
h_c / D_c	0.0416	0.0625	0.0579	0.10416	0.125	N/A
$R_{Sensitivity}$, on h_c/D_c	1	1	N/A	1	1	1
K_b (Bending)	0.95	1.425	1.90	2.375	2.85	N/A
h_c / D_c	0.0416	0.0625	0.0579	0.10416	0.125	N/A
$R_{Sensitivity}$, on h_c/D_c	1	1	N/A	1	1	1

The K_t and K_b are both hence sensitive to the change in the ratio of (h_c/D_c). Therefore, of the ratio of (h_c/D_c) in equation (29) and in equation (33) should not be considered a constant in the formulation of K_t. Thus, the sensitivity analysis cannot provide a simpler formulation of the K_t and K_b models, i.e. equation (29) and equation (33).

8 Discussion

The flexibility of the crankshaft of engines causes pronounced nonlinearities in their performance. Particularly, at crankshaft rotational speeds of about 2000 rpm and higher, the influence of the flexibility of crankshaft on the performance of the engine becomes relatively more pronounced. Such a higher frequency boosts these nonlinearities in the performance of the engine due to: (1) the increasing temperature that degrades the coolants [45]; (2) the operating frequency that becomes closer to the frequency of the maximum torque deliverable by the engine [46]; (3) the operating frequency that becomes closer to the frequency of the first mode of natural frequency of the engine [46]; (4) the non-linearity of the rate of fuel consumption [45]; (5) the non-linearity of the rate of exhaust emissions which is in turn due to the non-linearity of the rate of fuel consumption [45]; (6) the higher turbulent flow of the mixed phase fluids inside the engine [45]; (7) the more intense heat transfers of mixed modes within the cylinder head [45]; (8) the ignition delays [45].

The flexibility of crankshaft has an impact on the air quality, since it decreases the mass flow rate of air, so that the CO exhaust emissions become unfavorably higher [47]. The present study has hence presented analytical modeling of the energy-based aspects, frequency-related aspects and stress concentration in diesel engines with flexible crankshaft. The torsional stress and bending stress are the significant stresses developed in the crankshaft during its operations, and hence are the considered types of stresses in the analysis of the

stress concentration in the crankshaft [48, 49]. Since the proposed model is analytical and follows from the principles of physics, it is physically explainable and embodies a self-validated approach. The effect of the flexibility of the crankshaft on the resulting forces and provided energy is less than 1% and is thus insignificant, as can be gathered from equations (9) and (14). It has been found that the radial force in the crankshaft is several times larger than the tangential force. The force due to cylinder's pressure is several times larger than the force due to inertia, which is in turn several times larger than the force due to eccentricity.

The model of the strain energy in the crankshaft (U_{Total}) taking the flexibility of the shaft into consideration has been provided in equation (23). The sensitivity analysis that has been conducted on this analytical model, as shown in Table 1, indicates that the U_{Total} is sensitive to the change in E_c, L_A, L_B, R_{crank}, η_{bt}, T_{max}, Gc, Jc, and Ic. Hence, equation (23) is actually the simplest analytical model of the strain energy in the flexible crankshaft (U_{Total}). According to Table 1, the most influential factors onto the strain energy of flexible crankshafts are the mass moment of inertia of the shaft (I_c) and the distance between the crank and the bearing of the shaft (L_A). The developed analytical model of the U_{Total} has been validated using a case study that is indicated in Table 2. The statistical analysis based on the ε_R has shown 8% deviation from the bench mark, as shown in Table 3. Such a value of relative error is better than the relative error associated with the widely known CMEM model that indicates deviation of more than 10% from field data [50, 10]. In addition, such a relative error of 8% is on par with the relative error associated with the widely known GT-Power modeler [51]. It is noteworthy that the line of reasoning in developing the analytical models of the forces pertinent to the crankshaft, i.e. equations (3) through (15), is basically in accord with several other research papers in this research area, such as [52, 53]. In fact, the analytical sub-models developed for deriving the analytical model the U_{Total} of equation (23) produce a basically similar trend of results to the results in relevant papers, such as [52], in which the resulting radial force acting on the crankshaft is larger than the corresponding tangential force. Such a widely valid model would help in better analyzing the performance of diesel engines and in improving air quality.

The study proposed in section 6 an effective approach to remedy the stress concentration in the most critical section in crankshaft by identifying: (i) the location of the most critical section of stress concentration in crankshaft, (ii) the effect of the radius of the crankpin shoulder fillet (r_c) on the maximum shearing stress (τ_{ave}) and the maximum bending stress (M_{ave}) that can be carried by the crankpin in the most critical section in the crankshaft. Such a physically explainable model would help in the design of crankshafts of relatively long fatigue life. The present study has facilitated the determination of the value of the radius of the crankpin shoulder fillet that remedies the stress concentration in the most critical section of stress concentration in crankshaft. This would help in better prolonging their service life of diesel engines. The present study has also analyzed how sensitive the stress concentration factors (K_t) and (K_b) are to the change in independent variables, as indicated in Table 5, proving such sensitivity of the K_t and the K_b to the ratio of (h_c/D_c). Hence, the ratio of (h_c/D_c) in equations (29) and (33) should not be considered a constant in the formulation of K_t and K_b respectively. Therefore, equations (29) and (33) are the simplest analytical models of the K_t and the K_b. This sensitivity can be remedied by adopting crankshafts made of efficient structural material. Actually the macroscopic loading translates at the nano-scale at the end of the day into two types of stress: normal stress and shear stress. Recently nanotubes have been proposed for structural strengthening elements into the alloy structure of some vehicular parts. For each type of nano-scale stress, the nano-I-beam is exceptionally superior, outperforming the nanotube, due to its exceptional geometry [54]. Thus, the nano-I-beam can be utilized in the alloy structure of the structural steel of the crankshaft for reducing induced stresses and therefore prolonging the service life of the shaft. Also, the nano-I-beam can be used as nano-fibers in nano-composite-based crankshafts either based on organic or inorganic elements for reducing induced stresses and hence prolonging the service life of the crankshaft. The present models developed in the present study would help in analyzing the performance of not only compression ignition engines that operate on conventional diesel fuel, but also on the promising and sustainable compression ignition engines that operate on bio-fuel [55-57], or possibly on Hydrogen [11].

The future research horizon in this field is vastly wide. Amongst the promising technologies in which the further development of research on crankshaft may be promising are the hydrogen-based internal combustion engines and fully bio-fuel-based engines. Further experimental validation of the proposed analytical models can be sought for the engines of these environmentally friendly technologies. This is particularly in line with the current tendency of increasing the cylinder pressure towards increasing the efficiency of the combustion engines. Future research may investigate whether increasing the in-cylinder pressure would negatively affect

tribologically the building-up and development of the lubricating oil film thickness in flexible crankshafts and piston/cylinder assembly in such future technology engines. Further advanced materials of efficient nano-structures, such as nano-composites based on the nano-I-beam, could be sought as the structural material of future crankshaft and engines, exhibiting lighter weight and longer service life. In addition, further optimization endeavors could be sought for realizing a more streamlined design of the crankshaft for minimizing the current stress concentration at the discontinuity between crank pin and crank cheek in flexible crankshafts.

The implications of the present results can influence the crankshaft design practices in the automotive industry. The automotive crankshaft market is expected to reach an estimated \$3.2 billion by 2030 with a Compound Annual Growth Rate (CAGR) of 2.1% from 2024 to 2030 [58]. This expected growth of the automotive crankshafts market is fuelled by: (i) New trend of increasing the pressure in the cylinders of diesel engines for improved efficiency and performance [11, 59]; (ii) New trend of using renewable energy hydrogen internal combustion engines; (iii) New trend of using advanced materials such as nanomaterials like Carbon nanotubes and/or the more mechanically and thermodynamically efficient Carbon nano-I-beams [54, 59]. Thus, there is an increase in demand for performance engines, which indicates an increase in demand for engines development and innovative designs of crankshafts. Therefore, there is a need for facilitating to reach the optimum design of crankshafts for internal combustion engines. The present paper provides design guidelines that can facilitate the optimization of the crankshaft for slashing the risk and issue of fatigue failure and wear in crankshafts, in order to ensure long service life of engines. Asia and Asia-Pacific comprise fast emerging economies and have significantly higher demand than other regions for heavy commercial vehicles, buses, and high-end luxury vehicles (in the levels of features, comfort, and equipment) along with others vehicles.

Since the crankshaft is the key component of the modern internal combustion engines, the expected growth in the global automotive crankshafts market size is expected to trigger an era of improving developments in the crankshaft technology led by some automakers. Several automakers have been working on improved design and technology of crankshafts. The proposed design guidelines in the present paper can facilitate these potential developments for slashing the risk and issue of fatigue failure and wear in crankshafts, in order to ensure long service life of engines. Starting from the last decade, the knife edge crank technology has been used extensively in crankshafts. In this knife-edging process, the counterweights on the crankshaft are sharpened, in order to promote the process of cutting through the oil path in the pan. This cut through the oil path in the crankcase results in less restriction on the lubrication flow and thus reduced friction and wear. In 2020, Honda started the development of a 3D printed metal crankshaft, designed to reduce the vehicular weight and to improve the fuel efficiency [60]. Honda aims at scaling up the design and production of this crankshaft technology in the next few years. In 2021, in its high-performance cars series M3 and M4 with naturally-aspirated engines, BMW introduced improved material for the forged crankshaft using chrome molybdenum heat-treated alloy steel. In addition, BMW introduced new design of crankshafts in which crankpins are connected spherically, in order to allow the bearings to move more smoothly [60].

9 Conclusion

The present study has reported the following conclusions:

1. Analytically modeled the strain energy in the flexible crankshaft (U_{Total}), as presented in eqn. (23) in section 3;

2. Simplifying the model for control applications based on the sensitivity analysis of the analytically modeled strain energy, as presented in section 4;

3. Validated the flexible crankshaft's strain energy model with a relative error of 8%, as presented in section 5;

4. Proposed in section 6 to remedy the stress concentration in the most critical section in crankshaft by identifying: (i) the location of the most critical section of stress concentration in crankshaft, (ii) the effect of the radius of the crankpin shoulder fillet on the maximum shearing stress that can be carried by the crankpin;

5. Facilitated in section 6 the determination of the value of the radius of the crankpin shoulder fillet that remedies the stress concentration in the most critical section of stress concentration in crankshaft;

6. Showed the sensitivity analysis of the stress concentration factor (K_t), as can be gathered from section 7.

The results show that the most influential parameters onto the strain energy of flexible crankshafts are the mass moment of inertia and the distance between the crank and the bearing of crankshaft. The radial force in the crankshaft is several times larger than the tangential force. The force due to cylinder's pressure is several times larger than the force due to inertia, which is in turn several times larger than the force due to eccentricity. The present paper investigated the failure mechanisms, the identification of the failure's root causes, and the proposal of preventive actions to avoid failures in vehicular crankshafts. The crankshaft's flexibility influences the resulting forces and the provided energy in the diesel engine by less than 1%. The crankshaft's flexibility therefore can affect the homogeneity/stratification of the charge in the Homogeneous charge compression ignition (HCCI) engines. The developed analytical models would help in better analyzing the performance of diesel engines, in prolonging their service life, and in environmentally improving air quality. These developed models would help in developing novel engines, such as the hydrogen-based internal combustion engines and fully bio-fuel-based engines.

The expected growth of the automotive crankshafts market is fuelled by: (i) New trend of increasing the pressure in the cylinders of diesel engines for improved efficiency and performance; (ii) New trend of using renewable energy hydrogen internal combustion engines; (iii) New trend of using advanced materials such as nanomaterials like Carbon nanotubes and/or the more mechanically and thermodynamically efficient Carbon nano-I-beams. Thus, there is an increase in demand for performance engines, which indicates an increase in demand for engines development and innovative designs of crankshafts. Therefore, there is a need for facilitating to reach the optimum design of crankshafts for internal combustion engines. The present paper provides design guidelines that can facilitate the optimization of the automotive crankshaft for slashing the risk and issue of fatigue failure and wear in crankshafts, in order to ensure long service life of engines.

Acknowledgments

References

[1] W.F. Faris, H.A. Rakha, S.A.M. Elmoselhy, "Analytical model of diesel engines exhaust NOx emission rate," *Int. J. Vehicle Systems Modelling and Testing,* vol. 9, no. 3/4, 2014.

[2] A. Milasinovic, I. Filipovic, A. Hribernik, "Contribution to the definition of the torsional stiffness of the crankshaft of a diesel engine used in heavy-duty vehicles," *Proc. IMechE Part D: J. Automobile Engineering,* vol. 223, pp. 921-930, 2009.

[3] L. Witek, F. Stachowicz, A. Zaleski, "Failure investigation of the crankshaft diesel engine," *Procedia Structural Integrity*, vol. 5, pp. 369-376, 2017.

[4] W. Kim, S. Lee, "Investigation of torsional vibration characteristics of marine diesel engine crankshaft system," *Proceedings of the 14th International Congress on Sound & Vibration (ICSV14), Cairns, Australia,* 2007.

[5] S. Saxena, R. Ambikesh, "Design and finite element analysis of connecting rod of different materials," *AIP Conference Proceedings,* paper # 020034, May 2021, doi: https://doi.org/10.1063/5.0049989.

[6] N. Bhise, M. Ramachandran, "Design and numerical evaluation of crankshaft of diesel engine for total deformation and strain," *Proceedings of the IOP Conference Series Materials Science and Engineering, Mater. Sci. Eng.* 810 012010, May 2020, doi: 10.1088/1757-899X/810/1/012010.

[7] M. Fonte, V. Infante, L. Reis, M. Freitas, "Failure mode analysis of a diesel motor crankshaft," *Engineering Failure Analysis,* vol. 82, pp. 681–686, 2017.

[8] L. Witeka, M. Sikora, F. Stachowicz, T. Trzepiecinski, "Stress and failure analysis of the crankshaft of diesel engine," *Engineering Failure Analysis*, vol. 82, pp. 703–712, 2017.

[9] E.G. Giakoumis, C.D. Rakopoulos, A.M. Dimaratos, "Study of crankshaft torsional deformation under steady-state and transient operation of turbocharged diesel engines," *Proc. IMechE, Part K: J. Multi-body Dynamics*, vol. 222, pp. 17-30, 2008.

[10] V.D. Chaudhari, D. Deshmukh, "Challenges in charge preparation and combustion in homogeneous charge compression ignition engines with biodiesel: A review," *Energy Reports*, vol. 5, pp. 960–968, 2019. doi: https://doi.org/10.1016/j.egyr.2019.07.008.

[11] S.A.M. Elmoselhy, W.F. Faris, H.A. Rakha, "Validated analytical modelling of supercharging centrifugal compressors with vaneless diffusers for H_2-biodiesel dual-fuel engines with cooled EGR," *International Journal of Hydrogen Energy*, vol. 42, no. 43, pp. 26771-26786, 2017, doi: http://www.sciencedirect.com/science/article/pii/S0360319917333967.

[12] H.A. Rakha, K. Ahn, W. Faris, K.S. Moran, "Simple vehicle powertrain model for modeling intelligent vehicle applications," *IEEE Trans. on Intelligent Transportation Systems*, vol. 13, no. 2, 2012.

[13] W.F. Faris, H.A. Rakha, S.A.M. Elmoselhy, "Supercharged diesel powertrain intake manifold analytical model," *Int. J. Vehicle Systems Modelling and Testing*, vol. 9, no.1, 2014.

[14] S.A.M. Elmoselhy, W.F. Faris, H.A. Rakha, "Experimentally validated analytical modeling of diesel exhaust HC emission rate," *Journal of Mechanical Science and Technology,* vol. 28, no. 10, pp. 4139-4149, 2014.

[15] H. Mei, L. Wang, M. Wang, R. Zhu, Y. Wang, Y. Li, R. Zhang, B. Wang, X. Bao, "Characterization of exhaust CO, HC and NOx emissions from light-duty vehicles under real driving conditions," *Atmosphere*, 12, 1125, 2021. doi: https://doi.org/10.3390/atmos12091125.

[16] S.V. Bohac, D.M. Baker, D.N. Assanis, "A global model for steady state and transient S.I. engine heat transfer studies", *SAE Transactions, Journal of Engines*, vol. 105, section 3, pp. 196-214, 1996, doi: https://www.jstor.org/stable/44736267.

[17] W. Chaing, L. Zhu, R. Patankar, "Mean value engine modeling and validation for a 4-stroke, single cylinder gasoline engine," *Trends in Applied Sciences Research*, vol. 2, pp. 124-131, 2007, doi: https://scialert.net/fulltext/?doi=tasr.2007.124.131.

[18] INRO Consultants, EMME/2 User's Manual, Release 8, Montreal, CA, INRO Consultants, 1996.

[19] S. Durrani, X. Zhou, A. Chandra, "Effect of vehicle mobility on connectivity of vehicular ad hoc networks," *Proceedings of the IEEE Vehicular Technology Conference (VTC2010-Fall), Canada*, 2010.

[20] F. An, and M. Barth, "Development of a comprehensive modal emissions model: operating under hot-stabilized conditions," *Transportation Research Record,* vol. 1587, pp. 52-62, 1997.

[21] S.A. Sulaiman, S.H.M. Murad, I. Ibrahim, Z.A. Abdul Karim, "Study of flow in air-intake system for a single-cylinder go-kart engine," *International Journal of Automotive and Mechanical Engineering*, vol. 1, pp. 91-104, 2010.

[22] E.F. Obert, Internal Combustion Engines and Air Pollution; Harper & Row Publishers, Inc., 1973.

[23] J.S. Souder, "Powertrain modelling and nonlinear fuel control," *M.Sc. Thesis, University of California, Berkley,* 2002.

[24] Y. Hongwei, Y. Jin, Z. Baocheng, "Analysis of the influences of piston crankshaft offset on piston secondary movements," *The Open Mechanical Engineering Journal,* vol. 9, pp. 933-937, 2015.

[25] N. Hailemariam, "Kinematics and load formulation of engine crank mechanism," Mechanics, Materials Science & Engineering Journal, 2015, (https://hal.science/hal-01305936/).

[26] S.N. Krivtsov, T.I. Krivtsova, A.S. Grebennikov, "Rotational dynamics of piston diesel engine crankshaft with deactivated cylinders at idle,"
IOP Conf. Series: Materials Science and Engineering 632, 012040 (2019) (doi:10.1088/1757-899X/632/1/012040)

27 Y. Huang, S. Yang, F. Zhang, C. Zhao, Q. Ling, H. Wang, "Non-linear torsional vibration characteristics of an internal combustion engine crankshaft assembly," *Chinese Journal of Mechanical Engineering,* vol. 25, no. 4, pp. 797-808, 2012, doi: 10.3901/CJME.2012.04.797.

[28] U.S. Environmental Protection Agency EPA, Process for conducting probabilistic risk assessment. Appendix A, RAGS Volume 3, Part A, Environmental Protection Agency EPA 2001.

[29] V. Fedák, P. Záskalický, Z. Gelvanič, Analysis of Balancing of Unbalanced Rotors and Long Shafts Using GUI MATLAB. Chapter 19 in the edited book: "MATLAB Applications for the Practical Engineer," InTech Open, pp. 535-564, 2014, doi: http://dx.doi.org/10.5772/58378.

[30] M.L. Baglione, "Development of system analysis methodologies and tools for modeling and optimizing vehicle system efficiency," PhD Thesis. University of Michigan, pp. 52–54, 2007, doi: hdl:2027.42/57640.

[31] J. Wasilewski, et al., "Evaluation of greenhouse gas emission levels during the combustion of selected types of agricultural biomass", *Energies*, 15, 7335, page 4, 2022, doi: https://doi.org/10.3390/en15197335.

[32] K. Vedat et al., "Calculation and Optimizing of Brake Thermal Efficiency of Diesel Engines Based on Theoretical Diesel Cycle Parameters," International Journal Of Engineering Technologies, Vol.2, No.3, 2016, page 102 (https://dergipark.org.tr/tr/download/article-file/225867)

[33] P. Wróblewski; G. Koszalka, An experimental study on frictional losses of coated piston rings with symmetric and asymmetric geometry. SAE International Journal of Engines, 14(6), 2021, doi: https://doi.org/10.4271/03-14-06-0051.

[34] P. Wróblewski, Analysis of torque waveforms in two-cylinder engines for ultralight aircraft propulsion operating on 0W-8 and 0W-16 oils at high thermal loads using the diamond like carbon composite coating. SAE Int. J. Engines, 15(1), 2022, doi: https://doi.org/10.4271/03-15-01-0005 .

[35] P. Wróblewski; R. Rogólski, Experimental analysis of the influence of the application of TiN, TiAlN, CrN and DLC1 coatings on the friction losses in an aviation internal combustion engine intended for the propulsion of ultralight aircraft," Materials, 14(22), 6839, 2021, doi: https://doi.org/10.3390/ma14226839 .

[36] J.G. Hawley, F.J. Wallace1, S. Khalil-Arya, "A fully analytical treatment of heat release in diesel engines," *Proc. Instn Mech. Engrs Part D: J. Automobile Engineering,* vol. 217, pp. 701-717, 2003.

[37] Ursus Company, "S-4003 engine specifications", see: https://www.tractordata.com/farm-tractors/009/3/5/9356-ursus-c-360-engine.html Accessed on 18-04-2022.

[38]   A. Milašinovi´c, Z. Milovanovic, D. Kneževi´c, I. Mujani´c, "Determination of differential equations of motion and parameters of an elastic internal combustion engine crankshaft," *Trans. FAMENA*, 40, pp. 83–95, 2016.

[39]   G. Keller, Statistics for Management and Economics. 9th ed.; South Western, Cengage Learning: Mason, OH, USA, 2012.

[40]   F.F. Beer, E.R. Johnston, J.T. Dewolf, D.F. Mazurek, Mechanics of Materials. 6th edition, McGraw Hill, 2012.

[41]   W.D. Pilkey, Formulas for Stress, Strain, and Structural Matrices. 2nd edition, John Wiley & Sons, Inc. Chapter 6, 2008.

[42]   EngineTeam, "Crankshaft Specifications of 2,3 JTD", KMotor Shop, EngineTeam Manual Version 3, 2023, doi: https://www.kmotorshop.com/document/shop/HK0185VR1/PI0031_ser.info_ver.3.pdf.

[43]   Centerline International, "Crankshaft and Connecting Rod Specifications", Centerline Alfa Products, 2023, doi: https://www.centerlinealfa.com/sites/centerlinealfa.com/assets/files/default/crank_specifications.pdf.

[44]   J.A. Collins, H.R. Busby, G.H. Staab, "Mechanical Design of Machine Elements and Machines: A Failure Prevention Perspective," Second Edition, John Wiley & Sons, Chapter 5, 2010.

[45]   G.L. Gissinger, R. Renard, M. Hassenforder, Model based design and control of diesel engines. *SAE International*, paper # 890568, 1989.

[46]   Y.H. Zweiri, J.F. Whidborne, L.D. Seneviratne, "Detailed analytical model of a single-cylinder diesel engine in the crank angle domain," *Proceedings of the Institution of Mechanical Engineers, Part D: Journal of Automobile Engineering,* vol. 215, no. 11, pp. 1197-1216, 2001.

[47]   S.A.M. Elmoselhy, W.F. Faris, H.A. Rakha, "Validated analytical modeling of diesel engines intake manifold with a flexible crankshaft," *Energies,* 14, 1287, 2021, doi: https://doi.org/10.3390/en14051287.

[48]   I.T. Jiregna1, G.G. Sirata, F.T. Soramo, "Fatigue failure analysis of crankshafts - a review," *International Journal of Innovative Science, Engineering & Technology (IJISET)*, vol. 7, no. 5, May 2020.

[49]   G. Devandran, L. Chee Wai, M. Hazim, M. Khalid, M. Hanis, "Design and development of five parallel engines for lubricants and fuel testing experimental rigs, Part 2," *The 2nd Integrated Design Project Conference (IDPC) 2015, Faculty of Mechanical Engineering, Universiti Malaysia Pahang*, December 2015.

[50]   H. Rakha, K. Ahn, A. Trani, "Comparison of Mobile5a, VT-Micro, and CMEM models for estimating hot stabilized light duty gasoline vehicle emissions," *Can. J. Civil Eng.,* vol. 30, pp. 1010–1021, 2003.

[51]   M. Bos, "Validation Gt-Power Model Cyclops Heavy Duty Diesel Engine," Master's Thesis, The Technical University of Eindhoven, Eindhoven, The Netherlands, 2007.

[52]   A.S. Mendes, L.F. Raminelli, M.P. Gomez, "Structural dimensioning of a crankshaft for a high power diesel engine," *SAE International*, SAE Paper # 2003-01-3530, 2003.

[53]   S. Ni, Y. Guo, B. Lv, D. Wang, W. Li, Z. Shuai, "Analysis of torsional vibration effect on the diesel engine block vibration," *Mechanics & Industry*, 21, 522, 2020, doi: https://doi.org/10.1051/meca/2020065.

[54]   S.A.M. Elmoselhy, "Hybrid organic/inorganic nano-I-beams for structural nano-mechanics," Nature, Scientific Reports, Article number: 18324, December 2019, doi: https://doi.org/10.1038/s41598-019-53588-2.

[55]   T.W.B. Riyadi, M. Spraggon, S.G. Herawan, M. Idris, P.A. Paristiawan, N.R. Putra, M. Faizullizam, R. Silambarasan, I. Veza, "Biodiesel for HCCI engine: prospects and challenges of sustainability biodiesel for energy transition," *Results in Engineering*, vol. 17, 100916, 2023, doi: https://doi.org/10.1016/j.rineng.2023.100916.

[56]   S.M. Rayapureddy, J. Matijošius, A. Rimkus, J. Caban, T. Słowik, "Comparative Study of

combustion, performance and emission characteristics of hydrotreated vegetable oil–biobutanol fuel blends and diesel fuel on a CI engine," *Sustainability*, vol. 14, no. 12, 7324, 2022, doi: https://doi.org/10.3390/su14127324.

[57] N. Geng, Y. Zhang, Y. Sun, "Location optimization of biodiesel processing plant based on rough set and clustering algorithm - a case study in China," *Engineering Review*, vol. 40, no. 3, 105-115, 2020, doi: https://er.riteh.hr/index.php/ER/article/view/1350.

[58] Lucintel's strategic growth consulting services, "Automotive Crankshaft Market Report: Trends, Forecast and Competitive Analysis to 2030", Lucintel's consulting services, 2024 (https://www.lucintel.com/automotive-crankshaft-market.aspx).

[59] S.A.M. Elmoselhy, W.F. Faris, H.R. Rakha, "Validated Analytical Modeling of Eccentricity and Dynamic Displacement in Diesel Engines with Flexible Crankshaft", Energies 2022, 15(16), 6083, (https://doi.org/10.3390/en15166083).

[60] Automotive Systems and Accessories Division, "Automotive Crankshaft Market Size, Share, Competitive Landscape and Trend Analysis Report, by Material, by Type and, by Vehicle Type : Global Opportunity Analysis and Industry Forecast, 2023-2032", Allied Market Research, Report Code: A13949, January 2025, (https://www.alliedmarketresearch.com/automotive-crankshaft-market-A13949).